

## **HIGHER ORDER EFFECTS IN BEAM-BEAM DEFLECTION\***

**Yu-Chiu Chao and Pisin Chen**

**Stanford Linear Accelerator Center,  
Stanford University, Stanford, CA 94309**

### **Abstract**

Beam-beam deflection scan is a useful tool, both in the SLC and in future linear colliders, for extracting information about the beam position, size and luminosity. This technique poses nontrivial challenges to the instrumentation in its own right. The understanding of all aspects of beam-beam deflection, in particular that of disruption, is therefore crucial to a successful implementation of this technique.

When disruption effects become strong mainly due to increased beam intensity per bunch, the simple rigid-bunch formula for beam-beam deflection is no longer valid. In this report we discuss the general modification to the rigid beam-beam deflection formula in the presence of disruption using various methods including analytical calculation, rigid and semi-rigid two-disk models, and simulation. The impact on the realistic beam-beam deflection in the SLC is also discussed.

Submitted to *Nuclear Instruments and Methods*

\*Work supported by Department of Energy contract DE-AC03-76SF00515.

## 1. Introduction

The method of beam-beam deflection scan employed in the Stanford Linear Collider (SLC) as a routine exercise to align colliding beams and determine beam sizes has matured considerably since the commissioning of the machine [1]. Its necessity becomes obvious when beam intensities are increased to the point where conventional wire scans are no longer practical, as is the case with SLC when the particle count per pulse exceeds  $1.0 \times 10^{10}$ . In proposed future linear colliders where the beam flux is even higher, beam-beam deflection may become one of the few viable options from which information can be drawn about beam sizes and luminosity.

Exactly because of the increasing importance of beam-beam deflection scan with higher beam intensity, it is crucial to address the problem of disruption effects in this context. At current SLC intensity, it is accurate enough to ignore disruption effects and employ the simple rigid bunch deflection formula.

$$\langle \phi \rangle_1 = \frac{-2r_e N_2}{\gamma} \frac{1}{\Delta} (1 - e^{-\frac{\Delta^2}{2\Sigma^2}}) \quad (1)$$

$$\Sigma^2 = \sigma_1^2 + \sigma_2^2 ,$$

where  $\langle \phi \rangle$  is the deflection angle of the centroid of the beam,  $r_e$  is the classical electron radius,  $\gamma$  is the relativistic factor,  $\Delta$  is the impact parameter, and  $\sigma$  is the transverse rms beam size. The subscripts 1 and 2 label the two colliding beams.

At higher beam intensity, colliding bunches steer and deform each other considerably throughout the course of the collision. Concurrent to the deflection process, the local beam distribution, and the deflecting forces

in turn, are significantly modified. This leads to a **highly** nonlinear deviation from the rigid deflection formula for which only low-order approximation or simulation techniques can be attempted. At sufficiently high disruption parameter  $D$ , to be defined later, this deviation has to be taken into account if information about beam size and luminosity is to be correctly extracted ~~from~~ it.

In this report we discuss various methods used in attempts at modeling this effect. The major mathematical difficulty in treating the problem lies in the inherent nonlinearity in the longitudinal dimension, exacerbated by ~~the~~ lack of symmetry in the transverse dimension which cannot be cleanly decoupled from the longitudinal one. In sec. 2 the problem is formulated and the rigid deflection formula briefly ~~reviewed~~. In sec. 3 an analytical ~~solution~~ solution is presented which takes full account of the transverse distribution in the absence of cylindrical symmetry, but addresses the nonlinearity in the longitudinal dimension only to the lowest order. In sec. 4 a conceptual two-disk model is discussed which focuses on the nonlinear aspects in the longitudinal dimension and offers predictions at various regimes of the impact parameter. However, this method is limited so far to rigid distributions in the transverse dimensions, and reflects only the dipole motion of the beam. This latter method is combined with simple multiparticle tracking to yield the results given in sec. 5, where the second moment of the transverse motion is included and **calculation** is made over the full range of the impact parameter. In sec. 6 results are given for full-fledged tracking, taking into account realistic optics of the SLC at various disruption parameters. Section 7 sums up the different methods and results.

## 2. Beam-beam deflection and the rigid deflection formula

In the current practice of beam-beam deflection scan in the SLC [2], electron and positron beams are directed against each other at an impact parameter  $A$  which steps through a predetermined range in typically 40 steps. The resulting deflected orbits of both beams are reconstructed using high resolution **BPMs**, and correlation between deflection angles and impact parameters is fitted to the rigid deflection formula **(1)** to extract information about beam sizes and luminosity. Figure **1** shows such a correlation. The deflection process is illustrated in fig. **2**. The two bunches head for collision at an impact parameter  $A$ . Their centroids coincide in the longitudinal dimension at time  $t = 0$ . For the rest of this report the following convention is adopted: Each beam possesses its own intrinsic co-moving *longitudinal coordinate* originating from individual bunch centroids while sharing the same *transverse axes* ( $x$  and  $y$ ) emanating from a common origin. The longitudinal axes ( $z_1$  and  $z_2$ ) point along the directions of motion of the individual bunches. Thus the two coordinate systems have opposite handedness. The two co-moving coordinates  $z_1$  and  $z_2$  taken on by any particle at any time  $t$  are related by  $z_1 + z_2 + 2t = 0$ , where the light velocity  $c = 1$  is implied. The rigid deflection formula **(1)** can be derived from such a setup by assuming Gaussian distributions in all dimensions. We can easily deduce the limiting cases of eq. (1):

$$\begin{aligned} \langle \phi \rangle_1 &= \left( -\frac{r_e N_2}{\gamma} \frac{\Delta}{\Sigma^2} \right) & \mathbf{A} \ll 2.23 \sigma , \\ \langle \phi \rangle_1 &= \left( -\frac{2r_e N_2}{\gamma} \frac{1}{\Delta} \right) & \mathbf{A} \gg 2.23 \sigma . . \end{aligned} \tag{2}$$

The quantity  $2.23 \sigma$  corresponds to the peak in the deflection curve in fig. 1.

### 3. Lowest order analytical calculation

We start by writing down a consistent set of equations relating the instantaneous beam distribution and the instantaneous deflection received by individual particles. A solution can be attained [3] for systems possessing certain simplicity and symmetry. It is however overambitious to attempt such a solution with realistic beam distributions and lack of transverse symmetry due to nonzero impact parameters.

Consider the colliding beam system in the framework of sec. 2 and fig. 2. A formulation of disruption effects in a cylindrically symmetric (i.e., zero impact parameter) system has been laid out in the discussion of luminosity enhancement in ref. [4] by Chen and Yokoya as follows, given the tri-Gaussian distribution

$$n_0(x, y, z) = n_{L0}(z)n_{t0}(x, y) = \frac{N}{\sqrt{2\pi}\sigma_z} e^{-\frac{z^2}{2\sigma_z^2}} \frac{1}{2\pi\sigma_x\sigma_y} e^{-\frac{x^2}{2\sigma_x^2}} e^{-\frac{y^2}{2\sigma_y^2}} \quad (3)$$

for each bunch, with  $N$  being the total number of particles per bunch, and the equation of motion for a particle in beam one acted upon by the EM force from beam two

$$\begin{aligned} \frac{d^2x_1}{dt^2} &= -\frac{4r_e}{\gamma} N_2 n_{L2}(z_2) \int \frac{(x_1 - x_2) n_{t2}(x_2, y_2)}{(x_1 - x_2)^2 + (y_1 - y_2)^2} dx_2 dy_2, \\ &= -\frac{4r_e}{\gamma} N_2 n_{L2}(-2t - z_1) \int \frac{(x_1 - x_2) n_{t2}(x_2, y_2)}{(x_1 - x_2)^2 + (y_1 - y_2)^2} dx_2 dy_2, \end{aligned} \quad (4)$$

$$\frac{d^2y_1}{dt^2} = -\frac{4r_e}{\gamma} N_2 n_{L2}(-2t - z) \int \frac{(y_1 - y_2) n_{t2}(x_2, y_2)}{(x_1 - x_2)^2 + (y_1 - y_2)^2} dx_2 dy_2,$$

where  $x_1$  and  $y_1$  are understood to be functions of both  $z_1$  and  $t$  and the formula of relativistic Coulomb scattering was used. In the presence of cylin-

drical symmetry, i.e., zero impact parameter, the Coulomb potential depends only on the transverse radius  $r$ , and we have

$$\begin{aligned}\frac{d^2 r_1}{dt^2} &= \frac{-4r_e N_2}{\gamma} n_{L2}(-2t - z_1) \frac{1}{r_1} \int_0^{r_1} n_{r2}(r') r' dr', \\ \frac{d^2 r_2}{dt^2} &= \frac{-4r_e N_1}{\gamma} n_{L1}(-2t - z_2) \frac{1}{r_2} \int_0^{r_2} n_{r1}(r') r' dr'.\end{aligned}\quad (5)$$

Notice that a reciprocal formula was written for the force due to beam one received by beam two, which in turn should give the variation in the transverse distribution  $n_{i2}$  of beam two as a function of  $t$  and  $z_2$ . The exact solution was to be obtained by consistently solving the coupled system of eqs. (5) while keeping in mind that  $r_1$  and  $r_2$  are functions of  $z$  and  $t$ . An iterative approach was adopted instead. The first equation of (5) was solved to lowest order in the sense that the  $r$  in the right-hand side of eq. (5) was replaced with the initial value  $r_{10}$ ,

$$\begin{aligned}r_1(t, z_1) &= r_{10} - \frac{4N_2 r_e}{\gamma} f_{10}(r_{10}) g(t, z_1), \\ f_{10}(r_1) &= \frac{1}{r_1} \int_0^{r_1} n_{r20}(r') r' dr', \\ g(t, z_1) &= \int_{-\infty}^t dt_1 \int_{-\infty}^{t_1} dt_2 n_{L2}(-2t_1 - z_1), \\ &= \int_{-\infty}^t dt_1 (t - t_1) n_{L2}(-2t_1 - z_1).\end{aligned}\quad (6)$$

Interchanging subscripts 1 and 2, we have the lowest order solution for beam two. This can then be used to obtain the lowest order deformation of beam two at any instant through the mapping from  $r_{20}$  to  $r_2$ :

$$n_{r2}^{(1)}(r_2, t, z_2) = n_{r02}(r_2) + \frac{4N_1 r_e}{\gamma} \left[ \frac{dn_{r02}}{dr_2} f_{02}(r_2) + n_{r02}^2 \right] g(t, z_2). \quad (7)$$

Notice that to this order the longitudinal and transverse dependencies are still separable.

In the current problem of beam-beam deflection, the cylindrical symmetry is lost due to the **nonzero** impact parameter. The formulation is therefore more involved. But the spirit of lowest order iteration will be followed.

-- First we notice that eq. (4) can be rewritten as

$$\begin{aligned} \frac{d^2 \vec{x}_1}{dt^2} &= \frac{-4r_e N_2}{\gamma} n_{L2}(-2t - z_1) \int \frac{\vec{x}_1 - \vec{x}_2}{|\vec{x}_1 - \vec{x}_2|^2} n_{t2}(\vec{x}_2) d\vec{x}_2, \\ &= \frac{-4r_e N_2}{\gamma} n_{L2}(-2t - z_1) \vec{\nabla}_1 f_2(\vec{x}_1), \end{aligned} \quad (8)$$

$$f_2(\vec{x}_1) = f_2(x_1, y_1) = \frac{1}{2} \int dx dy n_{t2}(x, y) \ln[(x_1 - x)^2 + (y_1 - y)^2],$$

where  $\vec{x}$  represents the two-dimensional vector  $(x, y)$ ,  $\vec{\nabla}$  the two-dimensional gradient operator  $(\partial/\partial x, \partial/\partial y)$ , and the relativistic Coulomb force is replaced, by the gradient of an equivalent line charge potential. This substitution turns out to be very helpful. Equation ( 8 ) is solved to the lowest order as in eq. (6):

$$\begin{aligned} x_1(t, z_1) &= x_{10} - \frac{4N_2 r_e}{\gamma} [\nabla_{1x} f_2(x_{10}, y_{10})] g(t, z_1), \\ y_1(t, z_1) &= y_{10} - \frac{4N_2 r_e}{\gamma} [\nabla_{1y} f_2(x_{10}, y_{10})] g(t, z_1), \end{aligned} \quad (9)$$

where  $g(t, z_1)$  is given in eq. (6). Equation (9) can then be inverted to the same (lowest) degree of accuracy to give

$$\begin{aligned} x_{10} &= x_1 + \frac{4N_2 r_e}{\gamma} [\nabla_{1x} f_2(x_1, y_1)] g(t, z_1), \\ y_{10} &= y_1 + \frac{4N_2 r_e}{\gamma} [\nabla_{1y} f_2(x_1, y_1)] g(t, z_1). \end{aligned} \quad (10)$$

Equation (10) can be used to derive the change in the distribution of beam one, due to the deflection given in eq. (9) through

$$n_{t1}^{(1)}(x_1, y_1, t, z_1) = \left| \frac{\partial(x_{10}, y_{10})}{\partial(x_1, y_1)} \right| n_{t01}(x_{10}, y_{10}). \quad (11)$$

where the superscript (1), which indicates the lowest order correction of the distribution, is included formally in  $n_{t1}^{(1)}$ . Calculating the Jacobian to first order and expanding  $n_{t01}$  around  $(x_1, y_1)$  gives

$$\begin{aligned} n_{t1}^{(1)}(x_1, y_1, t, z_1) &= n_{t01}(x_1, y_1, t, z_1) \\ &\quad + \frac{4N_2 r_e}{\gamma} g(t, z_1) \left[ n_{t01} \nabla_1^2 f_2 + (\vec{\nabla}_1 n_{t01}) \cdot (\vec{\nabla}_1 f_2) \right], \\ &= n_{t01} + \delta n_{t1}(x_1, y_1, t, z_1), \end{aligned} \quad (12)$$

where  $\delta n_{t1}$  sums up the deformation in the transverse distribution of beam one. Notice that this depends on the longitudinal coordinates, but the dependence is separable. The same formula applies to beam two, except for a *formally* different initial distribution since the two beams are not centered at the same point transversely. Adopting the transverse geometry as given in fig. 3, the transverse initial distributions of the two beams are

$$\begin{aligned} n_{01}(x_1, y_1) &= \frac{1}{2\pi\sigma_{1x}\sigma_{1y}} e^{-\frac{(x_1-\Delta)^2}{2\sigma_{1x}^2}} e^{-\frac{y_1^2}{2\sigma_{1y}^2}} \\ n_{02}(x_2, y_2) &= \frac{1}{2\pi\sigma_2\sigma_{2y}} e^{-\frac{x_2^2}{2\sigma_2^2}} e^{-\frac{y_2^2}{2\sigma_{2y}^2}} \end{aligned} \quad (13)$$

Given the lowest order change in the transverse distributions in eq. (12) for both beams, we can calculate the accumulated angular change of beam one, due to disruption. There are two contributions:

- (a) The net angular kick on beam one caused by the change in the transverse distribution of beam two.
- (b) The net angular kick on beam one caused by the change in the transverse distribution of beam one itself.

It can be shown that the two terms are identical up to a change of beam indices so that the sum of (a) and (b) is symmetric with respect to the two beams. The calculation of term (a) will be elaborated in the following.

Substituting  $\delta n_{t2}$  (obtained by interchanging subscripts 1 and 2 in eq. (12)) for  $n_{t2}$  in eq. (4) and then integrating over time, we get the net change in angle for a particle in beam one due to disruption in beam two

$$\begin{aligned}
\delta\phi_{1x}(x_1, y_1) &= \int_{-\infty}^{\infty} \delta \left( \frac{dx_1^2}{dt^2} \right) dt \\
&= - \frac{4r_e N_2}{\gamma} \int_{-\infty}^{\infty} dt n_{L2}(-2t - z_1) \\
&\quad \times \int \frac{(x_1 - x_2) \delta n_{t2}(x_2, y_2)}{(x_1 - x_2)^2 + (y_1 - y_2)^2} dx_2 dy_2 \\
&= - \left( \frac{4r_e}{\gamma} \right)^2 N_1 N_2 \int_{-\infty}^{\infty} g(t, z_2) n_{L2}(z_2) dt \\
&\quad \times \int \frac{(x_1 - x_2)}{(x_1 - x_2)^2 + (y_1 - y_2)^2} \left[ n_{t02} \nabla_2^2 f_1 + (\vec{\nabla}_2 n_{t02}) \cdot (\vec{\nabla}_2 f_1) \right] dx_2 dy_2, \quad (14)
\end{aligned}$$

where

$$\begin{aligned}
f_1 &= f_1(x_2, y_2) \\
&= \frac{1}{2} \int dx dy \frac{1}{2\pi\sigma_{1x}\sigma_{1y}} e^{-\frac{(x-\Delta)^2}{2\sigma_{1x}^2}} e^{-\frac{y^2}{2\sigma_{1y}^2}} \ln \left[ (x_2 - x)^2 + (y_2 - y)^2 \right].
\end{aligned}$$

It is shown in the Appendix that the integration over time yields a factor of  $\sigma_{z1}/(8\sqrt{\pi})$ . In eq. (14) we can use Green's identity in two-dimensions:

$$\int_A S \nabla^2 T da + \int_A (\vec{\nabla} S) \cdot (\vec{\nabla} T) da = \oint S \frac{\partial T}{\partial n} ds, \quad (15)$$

where  $S$  and  $T$  are functions over a two-dimensional area  $A$  and  $\partial/\partial n$  is the derivative with respect to the normal vector at boundary of  $A$ . The two-dimensional integral in eq. (14) can be rewritten (subscripts 1 and 2 are dropped for compactness) as:

$$\begin{aligned}
& \int \frac{(x_1 - x_2)}{(x_1 - x_2)^2 + (y_1 - y_2)^2} \left\{ n_0 \nabla^2 f + [\vec{\nabla} n_0 \cdot \vec{\nabla} f] \right\} dx_2 dy_2, \\
& = \int dx_2 dy_2 A(x_1, y_1, x_2, y_2) \left[ n_0 \nabla^2 f + (\vec{\nabla} n_0) \cdot (\vec{\nabla} f) \right], \\
& = \int dx_2 dy_2 \left[ (A n_0) \nabla^2 f + (A \vec{\nabla} n_0) \cdot \vec{\nabla} f + (n_0 \vec{\nabla} A) \cdot \vec{\nabla} f \right] \\
& \quad - \int dx_2 dy_2 \left[ n_0 \vec{\nabla} A \cdot \vec{\nabla} f \right], \\
& = \oint (A n_0) \frac{\partial f}{\partial n} ds - \int dx_2 dy_2 \left[ n_0 \vec{\nabla} A \cdot \vec{\nabla} f \right], \tag{16}
\end{aligned}$$

where

$$A(x_1, y_1, x_2, y_2) = \frac{x_1 - x_2}{(x_1 - x_2)^2 + (y_1 - y_2)^2}.$$

The surface integral can be dropped due to the asymptotic behavior of  $n_0$  at infinity. We are therefore left with an integral

$$\begin{aligned}
\delta\phi_{1x}(x_1, y_1) &= -\frac{\sigma_{z1}}{\sqrt{\pi}} \left( \frac{r_e}{\gamma} \right)^2 N_1 N_2 \int dx_2 dy_2 F(x_1, x_2, y_1, y_2), \\
F(x_1, x_2, y_1, y_2) &= \frac{1}{4\pi^2 \sigma_2^2 \sigma_1^2} e^{-\frac{x_2^2 + y_2^2}{2\sigma_2^2}} \\
&\quad \times \vec{\nabla}_2 \left( \frac{x_1 - x_2}{(x_1 - x_2)^2 + (y_1 - y_2)^2} \right) \cdot \vec{\nabla}_2 G(x_2, y_2), \\
G(x_2, y_2) &= \int dx dy e^{-\frac{(x-\Delta)^2 + y^2}{2\sigma_1^2}} \ln \left[ (x_2 - x)^2 + (y_2 - y)^2 \right], \tag{17}
\end{aligned}$$

where we assumed

$$\begin{aligned}
\sigma_{1x} &= \sigma_{1y} = \sigma_1, \\
\sigma_{2x} &= \sigma_{2y} = \sigma_2.
\end{aligned}$$

The evaluation of eq. (17) turns out to be quite difficult. It is however possible to evaluate the ensemble average of eq. (17), which is after all the interesting measurable quantity:

$$\langle \delta\phi_{1x} \rangle = \frac{1}{2\pi\sigma_1^2} \int dx_1 dy_1 e^{-\frac{(x_1-\Delta)^2+y_1^2}{2\sigma_1^2}} \delta\phi_1(x_1, y_1). \quad (18)$$

The lengthy evaluation of eq. (18) will not be reproduced in this report. We simply present the result here:

$$\begin{aligned} \langle \delta\phi_{1x} \rangle = & \left( \frac{D_2}{\sigma_{z2}} \frac{1}{\sqrt{\pi}} \right) D_1 \left\{ 2\sigma_2^2 \frac{1}{\Delta} \left[ e^{-\frac{\Delta^2}{2(\sigma_1^2+\sigma_2^2)}} - e^{-\frac{\Delta^2}{\sigma_1^2+2\sigma_2^2}} \right] \right. \\ & \left. - e^{-\frac{\Delta^2}{2\sigma_2^2}} 2\sigma_1^2 \int_0^\infty dr \frac{1}{r^2} I_1 \left( \frac{r\Delta}{\sigma_2^2} \right) Q(r, \sigma_1, \sigma_2) \right\}, \quad (19) \end{aligned}$$

where

$$\begin{aligned} Q(r, \sigma_1, \sigma_2) &= \left[ e^{-\frac{r^2}{2\sigma_2^2}} - 2 e^{-\frac{r^2}{2\Sigma^2}} + e^{-\frac{r^2}{2C^2}} \right], \\ \Sigma^2 &= \sigma_1^2 + \sigma_2^2, \\ C^2 &= \left( \frac{\sigma_1^2 \sigma_2^2}{\sigma_1^2 + 2\sigma_2^2} \right), \\ D_1 &= \frac{r_e N_1}{\gamma} \frac{\sigma_{z1}}{\sigma_1^2}, \\ D_2 &= \frac{r_e N_2}{\gamma} \frac{\sigma_{z2}}{\sigma_2^2}. \end{aligned}$$

The remaining integral in eq. (19) is well behaved, although no closed form can be found.  $I_1$  in eq. (19) is the Bessel function. The disruption parameters  $D_1$  and  $D_2$  are defined as in ref. [3]. They serve as a measure of the extent of the disruption effect. Despite the apparent quadratic dependence on  $D$  of eq. (19), it is actually the first order correction in  $D_1$  to the rigid deflection formula (1) as can be seen by taking the ratio of the two quantities.

The other half of the contribution to  $\langle \delta\phi_{1x} \rangle$ , namely that due to the change in the distribution of beam one itself, can be shown to be equal to eq. (19), with the following substitutions: *interchanging*  $\sigma_1$  and  $\sigma_2$  and *replacing*  $D_1$  by  $D_2$ .

The sum of these two contributions to  $\langle \delta\phi_{1x} \rangle$  is plotted in fig. 4 with nominal SLC parameters ( $\sigma_{1,2} = 2 \mu\text{m}$ ,  $D_{1,2} = 0.1$ ,  $\sigma_{z1,z2} = 1 \text{ mm}$ ). It has the correct qualitative behavior and predicts a modification to the rigid deflection formula by roughly 0.8% near  $\Delta = 0$ .

The approach developed thus far took into account the complete Gaussian distribution, and the solution does not rely on the presence of transverse symmetry. The compromise we have to make however is that the disruption effect, or the cross-interference between the beam distribution and the deflection force at successive stages of the bunch crossing, is developed only to the lowest order. As a result, the effect of disruption is not fully taken into account. In principle, if a certain convergence criteria is met the same program can be iterated with well defined physical meaning to obtain progressively more accurate solutions. Such a possibility is however quite remote, given the formidable algebra already present at the next iteration.

#### **4. Rigid two-disk model**

As mentioned in the previous section, the shortcoming of the lowest order analytical solution to eq. (4) is that the instantaneous change in the beam distribution under continuous kick from the other beam is not fully accounted for. In this section we introduce a conceptual model which helps,

highlighting the nonlinear nature of the problem and characteristic disruption effects at different regimes of the impact parameter.

Figures 5(a-c) depict a simplified picture of bunch collisions. The longitudinal distributions of the beams have been compressed into two b-function peaks  $2\sigma_z$  apart, each carrying a transverse Gaussian distribution with half of the total charge  $Ne$ . Again taking  $c = 1$ , the whole process of bunch crossing is concentrated in three steps corresponding to the coincidences of the “disks.” At each crossing the rigid deflection formula for transverse Gaussian distributions can be used to calculate the kick received by each disk, which in turn is used to propagate the disk rigidly to the next crossing point. In this idealized picture the mutual influence of the two beams and their immediate response can be analyzed in detail. Of course it takes further refinement before this model can be compared with reality. Insight into the nonlinear nature of the problem can be gained, however, by comparing this model against the rigid deflection formula.

#### 4.1 Small impact parameter: Suppression

In the following, all positions and angles  $x$  and  $x'$  refer to those of beam one, unless otherwise indicated. From fig. 5(b), since the transverse distributions are Gaussian, at  $t = 0$ , both front disks receive a kick according to eq. (2)

$$x'_{11} = - \frac{1}{4} \frac{r_e N}{\gamma \sigma_{\perp}} \frac{A}{\sigma_{\perp}} \quad (20)$$

where the subscript 11 denotes the kick received by the front disk due to the other front disk. The front disks then propagate with this new deflection angle to the next crossing point,  $t = \sigma_z$ , where the front disks meet the rear

disks of the other beam. By now the front disks have traveled a *transverse* distance of

$$x_{12} = \sigma_z x'_{11} = -\frac{1}{4} \frac{r_e N \sigma_z}{\gamma \sigma_{\perp}^2} \Delta = -\frac{1}{4} D \Delta, \quad (21)$$

and therefore the impact parameter has been reduced to  $A \times [1 - (1/4)D]$ .

Thus at  $t = \sigma_z$ , the kick is

$$x'_{12} = x'_{21} = -\frac{1}{4} \frac{r_e N}{\gamma \sigma_{\perp}} \frac{\Delta}{\sigma_{\perp}} \left(1 - \frac{1}{4} D\right), \quad (22)$$

and the total deflection received by the front disk is

$$x'_1 = x'_{11} + x'_{12} = -\frac{1}{2} \frac{r_e N}{\gamma \sigma_{\perp}} \frac{\Delta}{\sigma_{\perp}} \left(1 - \frac{1}{8} D\right). \quad (23)$$

The rear disk keeps propagating at an angle  $x_{12}$ . When the two rear disks cross at  $t = 2\sigma$ , the transverse position of the rear disk and the impact parameter are respectively

$$x_{22} = \sigma_z x'_{21} = -\frac{1}{4} D \Delta \left(1 - \frac{1}{4} D\right), \quad (24)$$

$$A' = \Delta + 2x_{22} = A \left(1 - \frac{1}{2} D + \frac{1}{8} D^2\right).$$

The  $A'$  given above induces a kick for the rear disk

$$x'_{22} = -\frac{1}{4} \frac{r_e N}{\gamma \sigma_{\perp}} \frac{A'}{\sigma_{\perp}} \left(1 - \frac{1}{2} D + \frac{1}{8} D^2\right), \quad (25)$$

and the total deflection received by the rear disk is

$$x'_2 = x'_{21} + x'_{22} = -\frac{1}{2} \frac{r_e N}{\gamma \sigma_{\perp}} \frac{A}{\sigma_{\perp}} \left(1 - \frac{3}{8} D + \frac{1}{16} D^2\right). \quad (26)$$

The deflection of the centroid of the two disks is just the average of eqs. (23) and (26). To first order in  $D$ , this is

$$x' = \frac{1}{2} \frac{r_e N}{\gamma \sigma_{\perp}} \frac{A}{\sigma_{\perp}} \left(1 - \frac{1}{4} D\right). \quad (27)$$

In the case of small initial impact parameter, the effect of disruption is a suppression of the rigid deflection result by a factor of  $(1 - D/4)$ . The suppression can be understood by looking at the deflection force experienced by a particle at a small impact parameter from the center of the oncoming beam distribution. The deflection force decreases with the impact parameter. Thus as disruption effect pulls the two beam centroids closer together, the effective deflection is reduced. Another interesting result is that if we consider the strong-weak model, namely only one beam is allowed to be disrupted while the other is assumed to have infinite inertia, the total deflection of the disrupted weak beam is just that given by eq. (23). Thus in this deflection regime, a strong-weak approximation yields only half of the total disruption effect.

Equation (27) shows that, with only transverse dipole motion taken into account, at  $D = 0.1$  the disruption effect modifies the rigid deflection formula by roughly 2.5%.

#### 4.2 Large impact parameter: Enhancement

In the other regime where the two beams are far apart transversely, we can repeat the previous exercise using the second formula in eq. (2).

At  $t = 0$ ,

$$x'_{11} = -\frac{r_e N}{\gamma} \frac{\mathbf{1}}{\Delta} \quad (28)$$

At  $t = \sigma_z$ ,

$$x_{12} = \sigma_z x'_{11} = -\frac{r_e N \sigma_z}{\gamma \sigma_{\perp}^2} \left( \frac{\sigma_{\perp}}{\Delta} \right)^2 \Delta,$$

$$\begin{aligned}
&= -D \left( \frac{\sigma_{\perp}}{\Delta} \right)^2 \Delta \\
\Delta' &= \Delta + x_{12} \\
&= \left[ 1 - D \left( \frac{\sigma_{\perp}}{\Delta} \right)^2 \right] \Delta \\
x'_{12} &= x'_{21} = -\frac{r_e N}{\gamma \sigma_{\perp}} \left( \frac{\sigma_{\perp}}{\Delta} \right) \left( 1 + D \left( \frac{\sigma_{\perp}}{\Delta} \right)^2 + \mathcal{O}(D^2) \right) . \quad (29)
\end{aligned}$$

Thus the total kick of the front disk is

$$x'_1 = \left( -\frac{2r_e N}{\gamma \sigma_{\perp}} \right) \frac{\sigma_{\perp}}{\Delta} \left[ 1 + \frac{1}{2} D \left( \frac{\sigma_{\perp}}{\Delta} \right)^2 \right] . \quad (30)$$

At  $t = 2\sigma_z$ ,

$$\begin{aligned}
x_{22} &= \sigma_z x'_{21} = -\frac{r_e N \sigma_z}{\gamma \sigma_{\perp}^2} \left( \frac{\sigma_{\perp}}{\Delta} \right)^2 \left[ 1 + D \left( \frac{\sigma_{\perp}}{\Delta} \right)^2 \right] \Delta , \\
&= -D \left( \frac{\sigma_{\perp}}{\Delta} \right)^2 \Delta - D^2 \left( \frac{\sigma_{\perp}}{\Delta} \right)^4 \Delta , \\
\Delta'' &= \Delta - 2x_{22} = \Delta \left[ 1 - 2 \left( \frac{\sigma_{\perp}}{\Delta} \right)^2 + \mathcal{O}(D^2) \right] , \\
x'_{22} &= -\frac{r_e N}{\gamma \Delta''} \\
&= -\frac{r_e N}{\gamma \Delta} \left[ 1 + 2D \left( \frac{\sigma_{\perp}}{\Delta} \right)^2 + \mathcal{O}(D^2) \right] . \quad (31)
\end{aligned}$$

Thus the total kick of the rear disk is

$$x'_{21} + x'_{22} = -\frac{2r_e N}{\gamma \sigma_{\perp}} \left( \frac{\sigma_{\perp}}{\Delta} \right) \left[ 1 + \frac{3}{2} D \left( \frac{\sigma_{\perp}}{\Delta} \right)^2 + \mathcal{O}(D^2) \right] . \quad (32)$$

Averaging over eqs. (30) and (32)

$$x^{\parallel} = -\frac{2r_e N}{\gamma \sigma_{\perp}} \left( \frac{\sigma_{\perp}}{\Delta} \right) \left[ 1 + D \left( \frac{\sigma_{\perp}}{\Delta} \right)^2 \right] . \quad (33)$$

Again this doubles the estimate by a strong-weak approximation. The effect of disruption in this regime is an enhancement. This is due to the fact that

at large impact parameters, the deflecting force decreases as  $\Delta$  is increased, although the rate of increase is not as pronounced as in the previous case.

### 4.3 Near maximum deflection: Shift of the peak

We are interested in the effect of disruption when  $\Delta$  is near the deflection peak since this will lead to a shift of the peak which can serve as a visible signature of disruption. From the result of secs. 4.1 and 4.2, it is expected that the peak will shift outward under disruption. We can check this by repeating the same exercise once more, this time using an expansion formula of eq. (1) around the peak ( $\Delta \approx 2.23 \sigma$ ):

$$\langle \phi \rangle = -\frac{2D\sigma_{\perp}}{\sigma_z} \left[ A - B \frac{(\Delta - d)^2}{\sigma^2} \right], \quad (34)$$

$$d = 2.23\sigma, \quad A = 0.3190, \quad \text{and} \quad B = 9.7160 \times 10^{-2}.$$

Equation (34), which approximates the deflection curve around the peak with a parabola, will be used to calculate the shift of the peak due to a linear term caused by disruption.

At  $t = 0$ ,

$$x'_{11} = -\frac{D\sigma}{\sigma_z} \left[ A - B \frac{(\Delta - d)^2}{\sigma^2} \right]. \quad (35)$$

Remember that only half of the charge is on each disk.

At  $t = \sigma_z$ ,

$$\begin{aligned} x_{12} &= x'_{11}\sigma_z, \\ &= -D\sigma \left[ A - B \frac{(\Delta - d)^2}{\sigma^2} \right], \end{aligned}$$

$$\Delta' = \Delta + x_{12},$$

$$\begin{aligned}
&= d + \delta - D\sigma \left[ A - B \frac{(\Delta - d)^2}{\sigma^2} \right], \quad \text{where } \delta = \Delta - d, \\
x'_{12} = x'_{21} &= -\frac{D\sigma}{\sigma_z} \left\{ A - \frac{B}{\sigma^2} \left[ \delta - D\delta \left( A - \frac{B\delta^2}{\sigma^2} \right) \right]^2 \right\} \\
&= -\frac{D\sigma}{\sigma_z} \left[ \left( A - \frac{B\delta^2}{\sigma^2} \right) \left( 1 + \frac{B}{\sigma} 2\delta D \right) - D^2 A^2 B \right]. \quad (36)
\end{aligned}$$

Thus the total kick of the front disk is

$$x'_1 = -\frac{2D\delta}{\sigma_z} \left[ \left( A - B \frac{\delta^2}{\sigma^2} \right) \left( 1 + D \frac{B\delta}{\sigma} \right) - \frac{1}{2} D^2 A^2 B \right]. \quad (37)$$

At  $t = 2\sigma_z$ ,

$$\begin{aligned}
x_{22} &= \sigma_z x'_{21}, \\
&= -D\sigma \left[ \left( A - \frac{B\delta^2}{\sigma^2} \right) \left( 1 + 2D \frac{B\delta}{\sigma} \right) - D^2 A^2 B \right], \\
\Delta'' &= \Delta + 2x_{22}, \\
&= \Delta - 2D\sigma \left[ \left( A - \frac{B\delta^2}{\sigma^2} \right) \left( 1 + 2D \frac{B\delta}{\sigma} \right) - D^2 A^2 B \right], \\
x'_{22} &= -\frac{D\sigma}{\sigma_z} \left[ \left( A - \frac{B\delta^2}{\sigma^2} \right) \left( 1 + \frac{4B}{\sigma} D\delta \right) - 4D^2 A^2 B \right] + \mathcal{O}(D^3). \quad (38)
\end{aligned}$$

Thus the total kick of the rear disk is

$$x'_2 = -\frac{2D\sigma}{\sigma_z} \left[ \left( A - \frac{B\delta^2}{\sigma^2} \right) \left( 1 + 3 \frac{B}{\sigma} D\delta \right) - \frac{5}{2} D^2 A^2 B \right]. \quad (39)$$

Averaging over eqs. (37) and (39),

$$x' = -\frac{2D\sigma}{\sigma_z} \left[ \left( 1 + 2 \frac{B}{\sigma} \delta D \right) \left( A - B \frac{\delta^2}{\sigma^2} \right) - \frac{3}{2} D^2 A^2 B \right]. \quad (40)$$

Once more, this gives twice the contribution of a strong-weak approximation.

Inspecting eq. (40) we see that the peak of the original parabola has been

shifted by the term linear in  $\delta$ . To first order in  $D$ , we have the new curve given by

$$\begin{aligned} x' &= -\frac{2D\sigma}{\sigma_z} \left( A + \frac{2ABD}{\sigma} \delta - B \frac{\delta^2}{\sigma^2} \right) \\ &= -\frac{2D}{\sigma_z} \left\{ \frac{B}{\sigma} A + 2\sigma AD\delta - \delta^2 \right\}. \end{aligned} \quad (41)$$

This implies that the peak of the parabola has been shifted from  $\delta = 0$  to  $\delta = AD\sigma$ . Therefore

$$\frac{\{\text{Shift of peak}\}}{\sigma} = AD = 0.3190 D. \quad (42)$$

Figure 6(a) shows the qualitative effect of disruption incorporating all the signatures discussed above. The dashed line represents the rigid deflection formula. Figure 6(b) shows the net effect of disruption inferred from fig. 6(a). Notice exactly the same characteristic was reflected in fig. 4, which came from the lowest order analytical calculation.

## 5. Semi-rigid two-disk model

The two-disk model developed in the previous section, while yielding intuitive insight, warrants ample room for refinement. First, one would prefer to include changes in the second moment in the transverse distribution to allow the “pinching” effect to manifest itself. Second, it is desirable to apply this model to cases other than the limiting ones discussed above. The first question can in principle be addressed using purely analytical tools. The second however is difficult short of resorting to numerical methods. A program is therefore developed which combines the analytical expression for single particle deflection and multiparticle tracking over a continuous range of impact parameters. The basic algorithm is described in the following.

As in the previous section, the longitudinal distributions are again compressed into two  $\delta$ -disks. The transverse distributions however become totally flexible by taking on a Gaussian distribution of a large number of particles, each one being allowed to move independently. The transverse kick a single particle receives from colliding with a Gaussian bunch at impact parameter  $\Delta$  is given by

$$\begin{aligned}\Delta\phi_x &= -\frac{2r_e N}{\gamma} \frac{\Delta_x}{\Delta^2} \left[ 1 - e^{-\frac{\Delta^2}{2\sigma^2}} \right], \\ \Delta\phi_y &= -\frac{2r_e N}{\gamma} \frac{\Delta_y}{\Delta^2} \left[ 1 - e^{-\frac{\Delta^2}{2\sigma^2}} \right].\end{aligned}\tag{43}$$

Adopting the same formulation as in the previous section, we use eq. (43) to calculate the kick received by each *individual* particle at each crossing. Each particle is propagated by its own slope independently to the next crossing point. Before the next kick is calculated, the transverse rms value as well as the centroid shift of the distribution is calculated, and new values of  $\Delta$  and  $\sigma$  inferred for each beam. The new  $\Delta$  and  $\sigma$  are then substituted into eq. (43) to calculate the next kick for each particle. This is repeated throughout the course of crossing.

Figure 7 shows such a calculation where the rigid deflection formula (1), the deflection of rigid two-disks (sec. 4), and that including second moment changes (this section) are compared. It is worth noting that the effect of change in second moment serves to counteract the effect due to the rigid two-disk model. This is especially significant at small  $\Delta$ . The reason lies in the pinching of the beam at small  $\Delta$ , which enhances the deflection and offsets the suppression due to centroid shift alone.

There appears to be plenty of room for augmenting this program. For example, the analytical formula for kick could be augmented by more complicated distribution both longitudinally and transversely, by inclusion of beam divergence (and therefore lattice optics), and so on. It is a promising approach, since it has the advantage of a tracking program while a considerable amount of number crunching is replaced by analytical formulas.

## 6. Tracking results

Tracking has been employed to simulate the disruption effect in the realistic SLC environment. In principle multiparticle tracking offers the ultimate standard against which the various methods developed above must be checked. It provides a granularity to a degree unmatched by the conceptual models, while taking into account the inherent nonlinearity and realistic optics, which are difficult for analytical methods. However, in reality, accuracy is limited by the computer capacity we can muster. In the current simulation, each beam has 20000 particles meshed into a  $32 \times 32$  grid transversely, and 100 compartments longitudinally. The statistics near the center of the distribution are decent enough to ensure stability against noise. Simulation was carried out for different disruption parameters  $D$ , and also for different optical conditions defined by the divergence parameter  $A$  given by [4]

$$A = \left( \frac{\sigma_z}{\beta^*} \right), \quad (44)$$

which is a measure of the inherent divergence of the beam, with  $\beta^*$  being the lattice beta at the collision point. A large  $A$  tends to complicate the disruption mechanism since the transverse size of the beam cannot remain constant throughout the collision. Figures 8(a,b) show tracking results for

different values of  $D$  and  $A$ , with  $D = 0.1$ ,  $A = 0.05$  corresponding to the current SLC running condition. The stability of the tracking is seen to be reasonable. We begin to suffer from limited computing power as the impact parameter is increased and the system steers farther away from cylindrical symmetry. To achieve better understanding of the disruption effects for a particular machine and to fully exploit its significance, further efforts must be made towards a more complete and refined set of tracking results.

## 7. Conclusion

In this report we have demonstrated different approaches that address the problem of disruption in beam beam deflection, with the SLC as a source of realistic parameters. Short of an analytical scheme which encompasses all the essential features of disruption at nonzero impact parameters, we settle for methods which focus on specific aspects of the problem. An analytical deflection formula was derived by considering the lowest order deformation of the source beam and the target beam separately. While yielding all the expected behaviors across the whole range of the impact parameter, the lowest order calculation stops short of touching on the nonlinear nature of the problem, and therefore is not expected to be accurate when  $D$  becomes large. One can expect to carry through such a program by iteration, thereby realizing the inherent nonlinearity. However the algebraic complexity poses a serious challenge to such attempts, as can be seen in the lack of decoupling in the longitudinal and transverse distributions at the next level of iteration.

The two-disk model presents a somewhat complementary approach to the analytical method. While the nonlinearity is addressed to some degree through the instantaneous feedback of the kick on the disk position,

the highly simplified picture discourages a serious association with reality beyond the conceptual level, neither does it provide much quantitative understanding outside the limiting regimes. It has been speculated that a more realistic longitudinal distribution be created by increasing the number of disks or even going to the continuous distribution, which should not present too much technical difficulty [5]. However, relaxing the rigid constraints in the transverse plane to a high order is much more involved.

Given the above considerations, the method presented in sec. 5, namely the tracking of semi-rigid disks, appears to be a very attractive alternative in that it keeps the advantage of the two-disk model while allowing more degrees of freedom to play in the transverse dimension. It also gives a quantitative picture across the whole range of the impact parameter. Computationally this method is much more efficient than pure multiparticle tracking because much of the number crunching has been replaced by analytical formulas, and many singular situations have been avoided due to the smearing of the deflecting force in these formulas. Currently, this method is being extended to smoothing out the longitudinal distribution, as well as including higher moments in the transverse dimension.

Full-fledged multiparticle tracking was also done in this study. As is true in all such practice in beam beam interactions, great care must be taken to ensure decent statistics and absence of singularity problems. This in turn translates into demands on computing power. With the specifics given in sec. 6, we obtained reasonable results pertaining to relevant SLC optics. The tracking result is seen to be stable against random fluctuations in the initial distribution.

The various methods employed in this report give results which agree to within **thesame** order of magnitude. Given the nominal parameters of the SLC, the disruption effect modifies the rigid deflection formula by less than 5.0%.

## **Acknowledgements**

We thank B. Richter and A. Hutton for suggesting this problem to us. Stimulating discussions with R. Ruth on the two-disk model and discussions with J. Irwin are also greatly appreciated.

## References

- [1] W. Koska et al., “Beam Beam Deflection as a Tuning Tool at the SLAC Linear Collider,” **Nucl. Instrum. Methods** A286 (1990) 32;  
R. Erickson, “Final Focus Systems for Linear Colliders,” **SLAC-PUB-4479** (1987).
- [2] W. Koska et al., op. cit.
- [3] P. Chen, “An Introduction to Beamstrahlung and Disruption,” in *Frontier of Particle Beams*, eds., M. Month and S. Turner, (Springer-Verlag, 1987).
- [4] P. Chen and K. Yokoya, “Disruption Effects from the Interaction of Round  $e^+e^-$  Beams,” **Phys. Rev. D-38 (1988) 987.**
- [5] J. Irwin, private communication.

**Appendix**  
**Calculating the time integral of perturbed**  
**longitudinal distribution**

We will evaluate the time integral in eq. (14)

$$\begin{aligned}
 I &= \int_{-\infty}^{\infty} g(t, z_2) n_{L2}(z_2) dt, \\
 &= \int_{-\infty}^{\infty} dt n_{L2}(-2t - z_1) \int_{-\infty}^t dt_1 (t - t_1) n_{L1}(-2t_1 + 2t + z_1),
 \end{aligned} \tag{A.1}$$

where  $n_{L2}(z_2)$  and  $g(t, z_2)$  are substituted from eqs. (3) and (6) respectively. The  $z_2$  is also replaced with  $-2t - z_1$ . Change the integration variables from  $(t, t_1)$  to  $(t, t - t_1)$  and the integration range accordingly, and we get

$$\begin{aligned}
 I &= \int_{-\infty}^{\infty} dt n_{L2}(-2t - z_1) \times \int_0^{\infty} dt t n_{L1}(2t + z_1), \\
 &= \frac{1}{2} \int_0^{\infty} dt t n_{L1}(2t + z_1).
 \end{aligned} \tag{A.2}$$

Now we take the ensemble average of this expression over the distribution  $n_{L1}(z_1)$ :

$$\langle I \rangle = \frac{1}{2} \int_{-\infty}^{\infty} dz_1 n_{L1}(z_1) \int_0^{\infty} dt t n_{L1}(2t + z_1), \tag{A.3}$$

with

$$n_{L1}(z) = \frac{1}{\sqrt{2\pi} \sigma_{z1}} e^{-\frac{z^2}{2\sigma_{z1}^2}}.$$

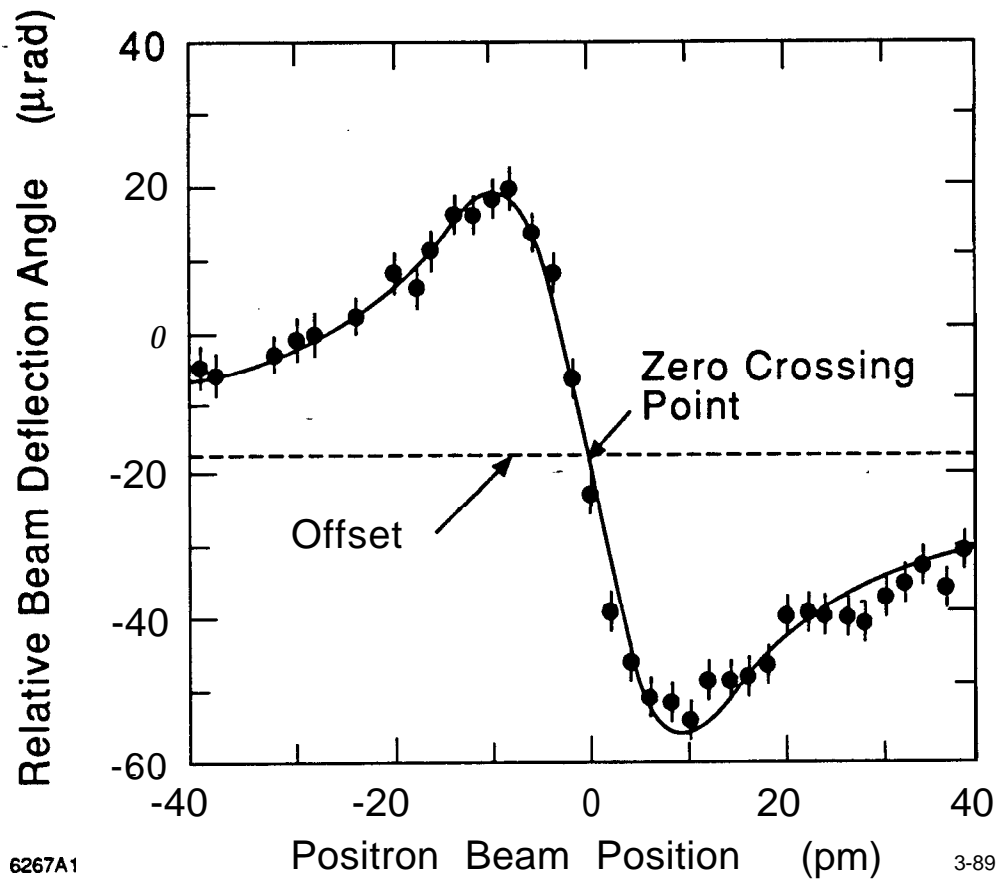
It's not hard to find that

$$\begin{aligned}
 \langle I \rangle &= \frac{1}{4\pi\sigma_{z1}^2} \int_0^{\infty} dt t \int_{-\infty}^{\infty} dz_1 e^{-\frac{z_1^2 + (z_1 + 2t)^2}{2\sigma_{z1}^2}} \\
 &= \frac{\sigma_{z1}}{8\sqrt{\pi}}
 \end{aligned} \tag{A.4}$$

## Figure Captions

1. A typical experimental observation of beam-beam deflection as seen in the SLC [1].
2. Longitudinal coordinate system used in the calculation of beam-beam deflection (see explanation in sec. 2).
3. Convention adopted in sec. 3 for the transverse dimension of the two-beam system.
4. Net disruption effect given by eq. (19) for  $D = 0.1$ . The horizontal axis is in units of the transverse beam sigma, while the vertical axis is in units of the quantity  $H_d = D \sigma_{\perp} / 2 \sigma_z$ .
5. Three steps of beam crossing in the two-disk model with increasing degree of complication:
  - (a) rigid disks with infinite inertia,
  - (b) first moment of disks allowed to change,
  - (c) second moment of disks allowed to change.
6. Qualitative modification of the rigid deflection formula inferred from the two-disk model (see sec. 4):
  - (a) rigid deflection formula (dashed) and deflection with disruption (solid),
  - (b) net effect of disruption.
7. Rigid deflection (solid), first moment effect (dashed), and second moment effect (dotted) for  $D = 1.5$  obtained by semi-rigid two-disk method (see sec. 5).

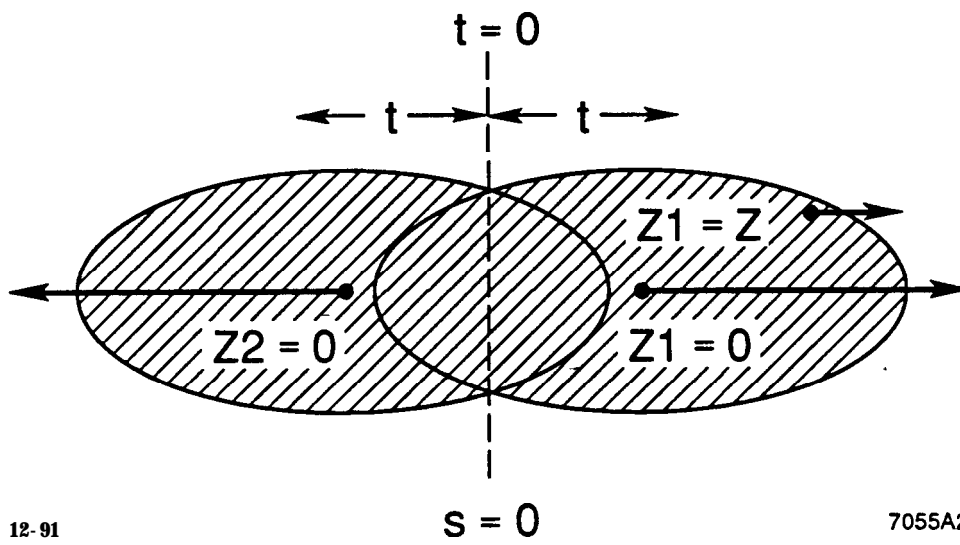
8. Tracking results for  $D = 0.01, 0.1$  and  $1.0$ . Dashed line represents rigid deflection formula. Some solid circles are overshadowed by hollow circles in cases of near coincidence.
- (a)  $A=0.0$ ,
  - (b)  $A=0.05$  (nominal SLC case).



6267A1

3-89

Fig. 1



12-91

7055A2

Fig. 2

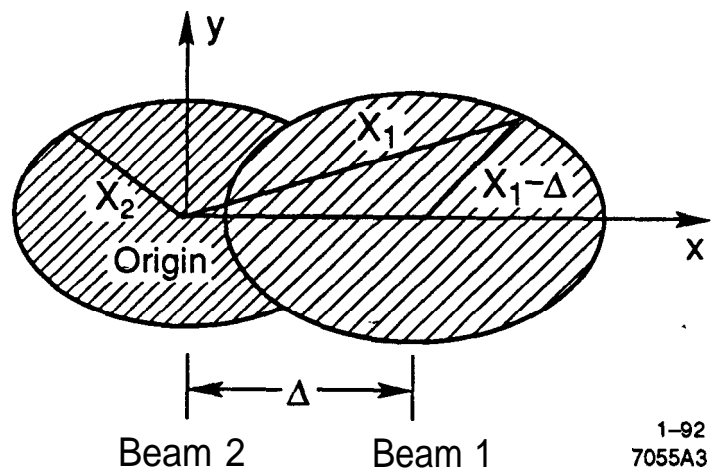
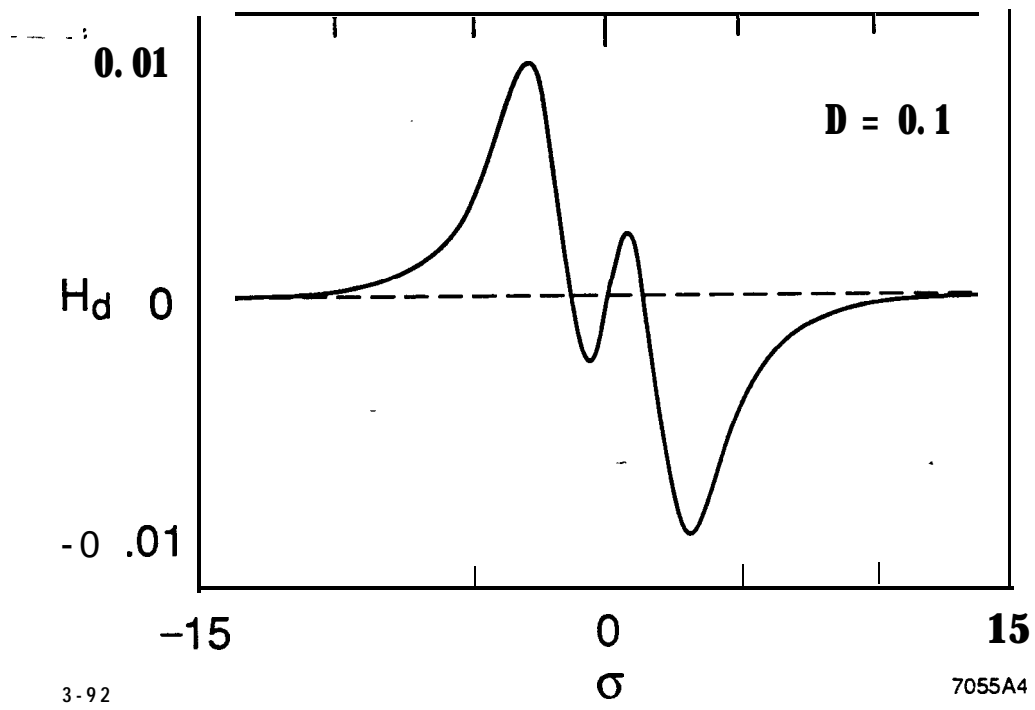


Fig. 3



3-92

7055A4

Fig. 4

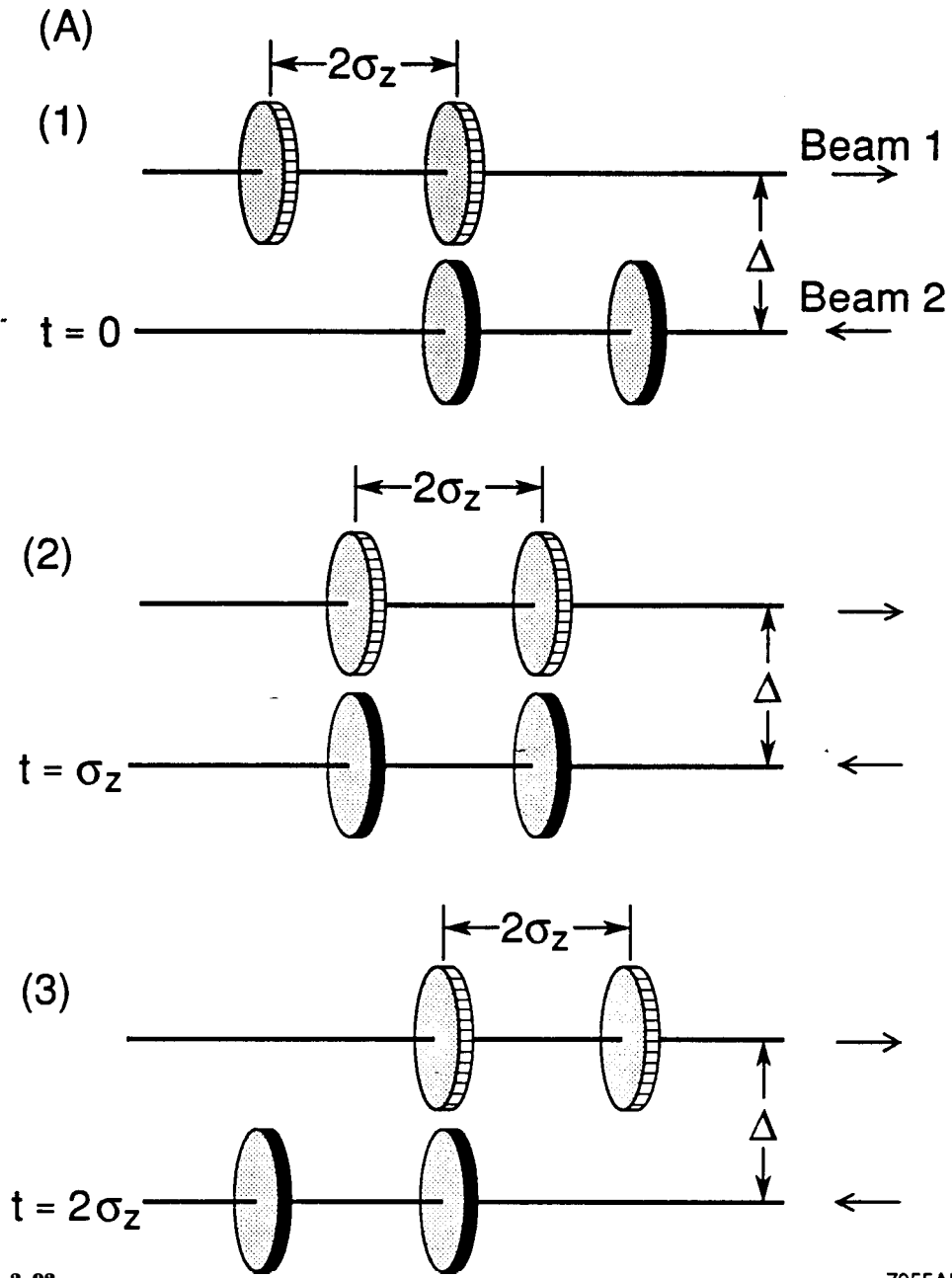


Fig. 5a

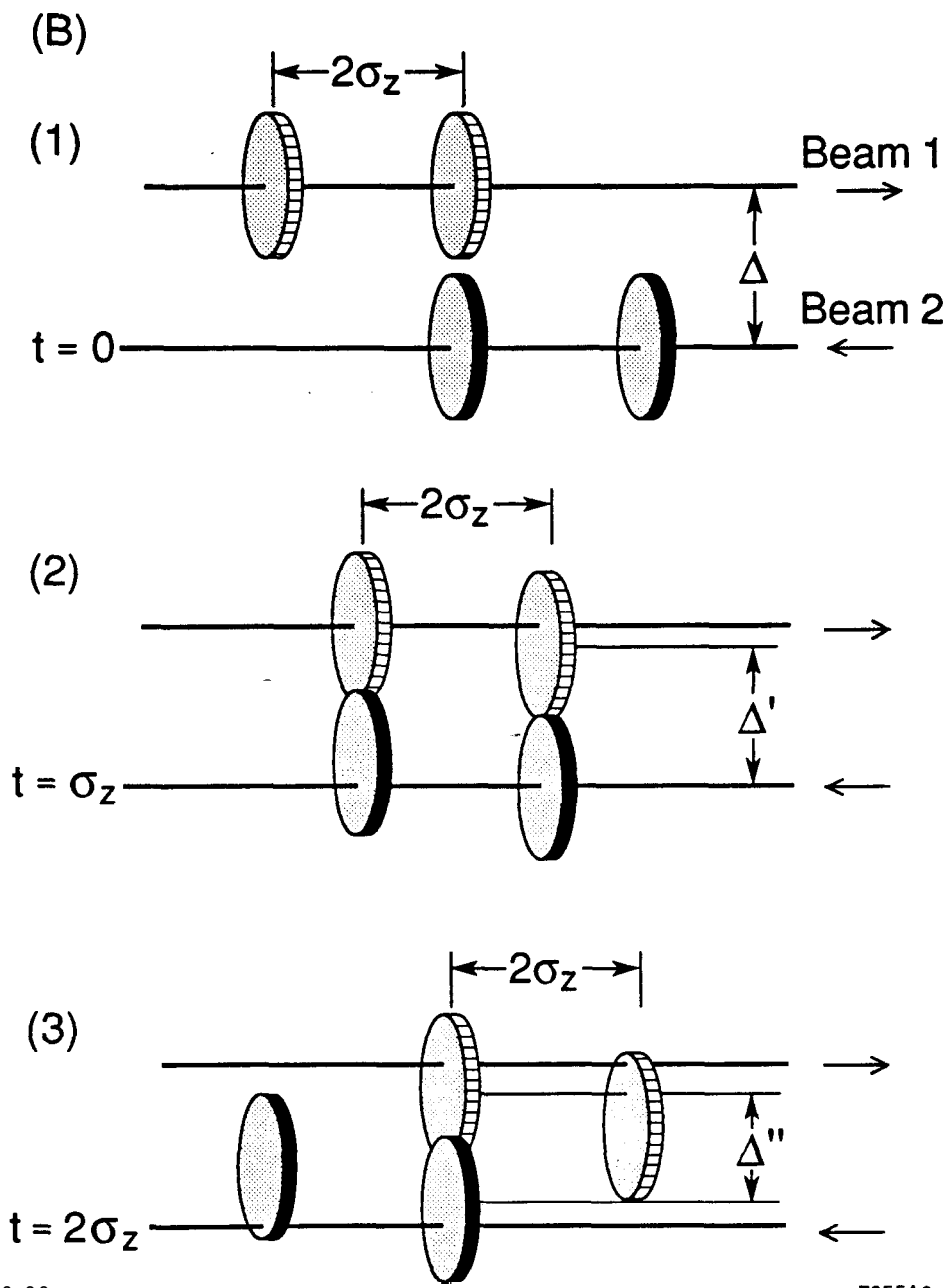


Fig. 5b

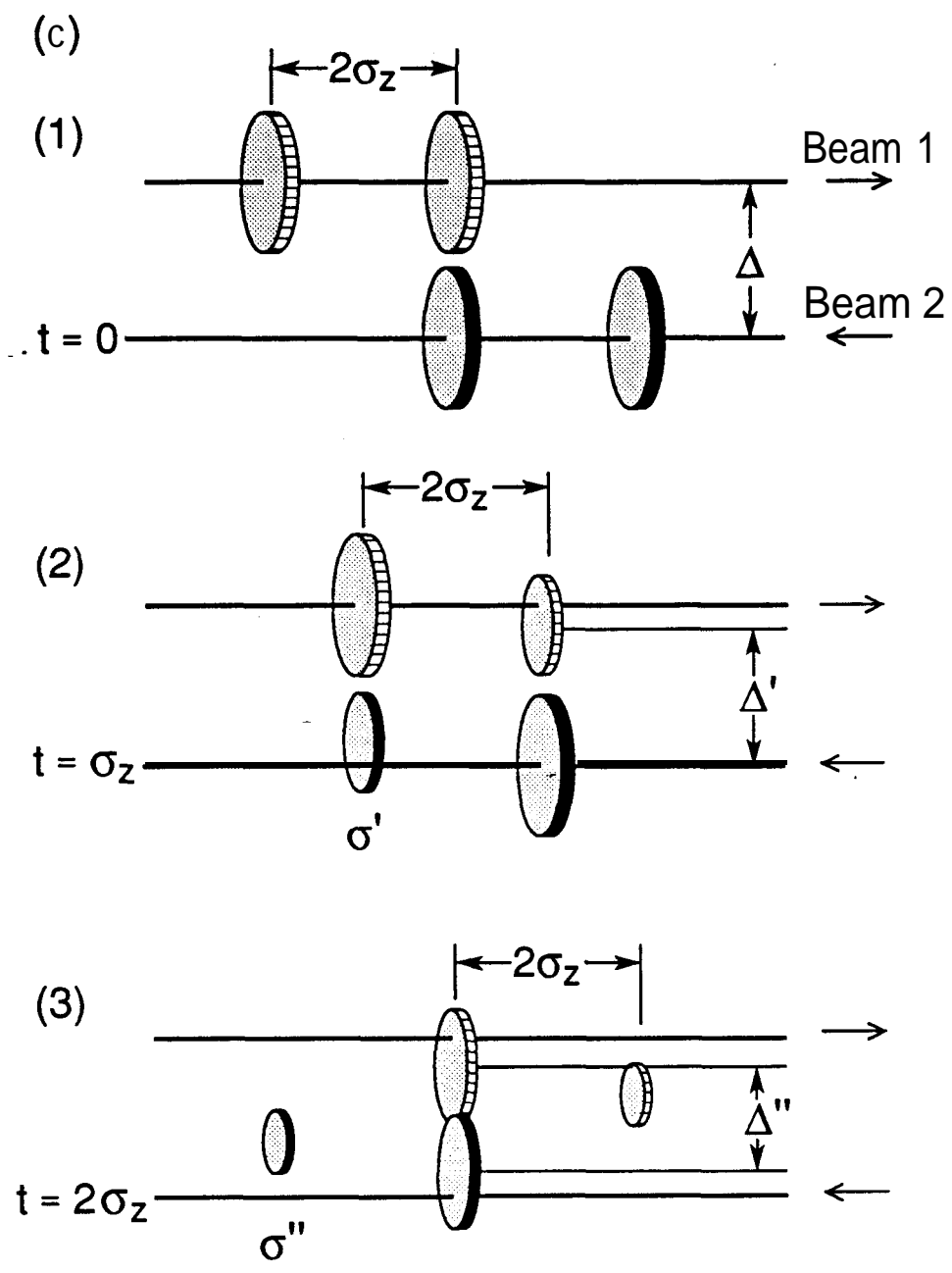


Fig. 5c

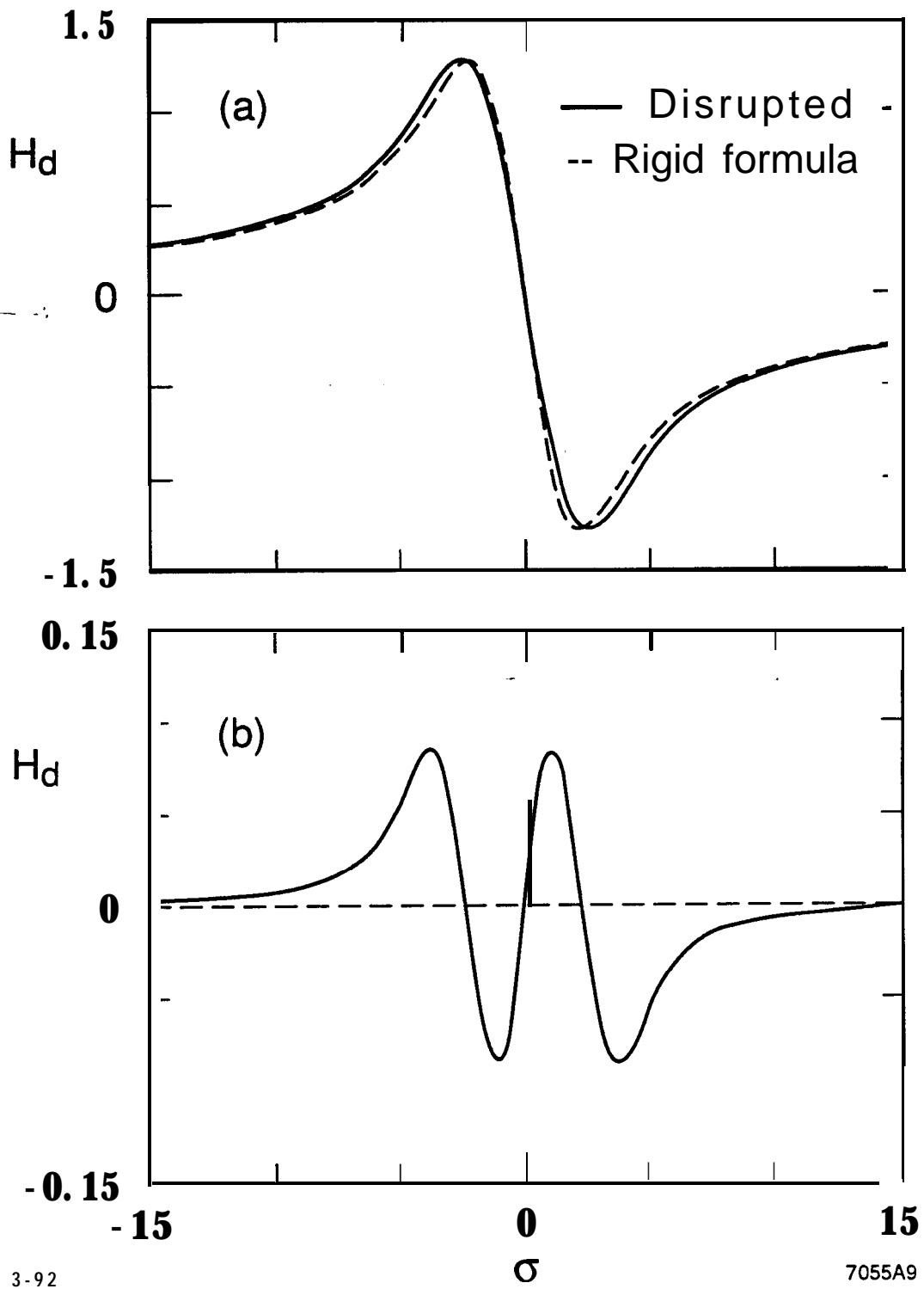


Fig. 6

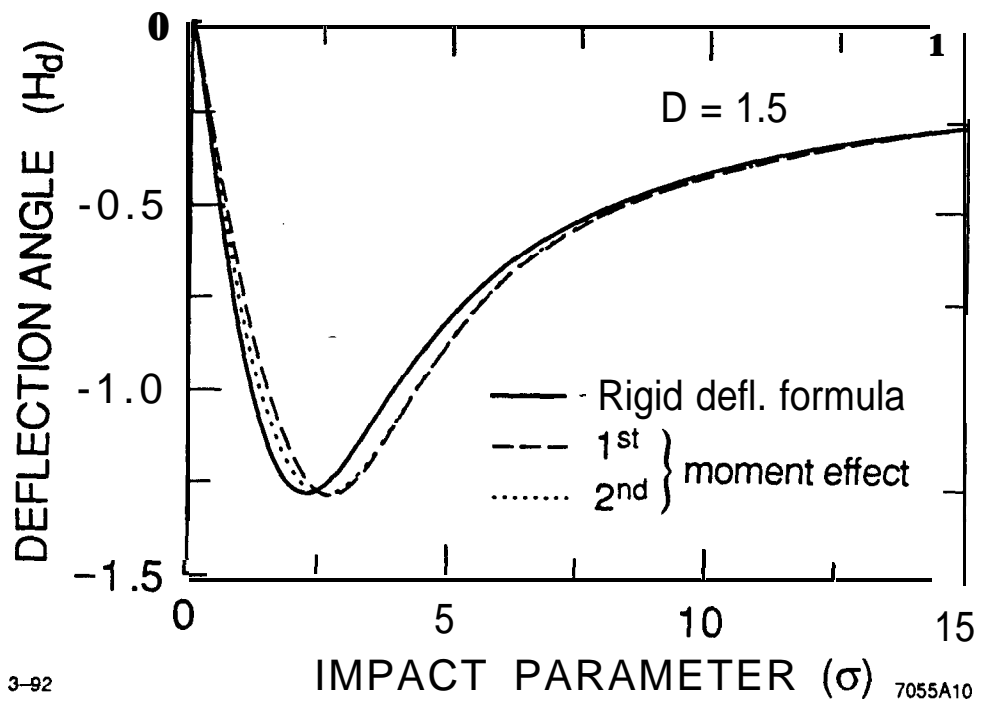


Fig. 7

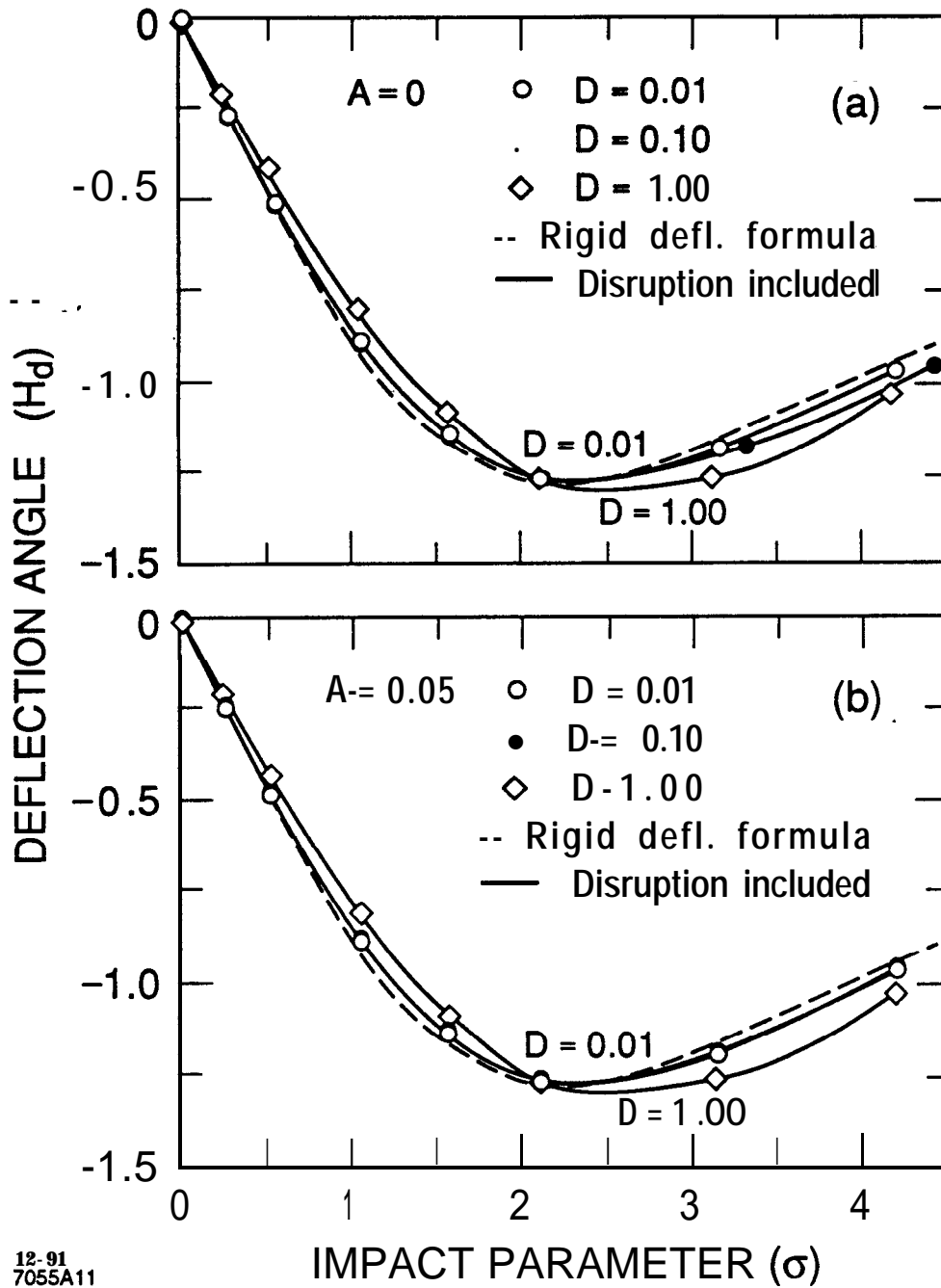


Fig. 8